



OPEN ACCESS

EDITED BY

Yongsheng He,
China University of Geosciences, China

REVIEWED BY

Yunchuan Zeng,
China University of Geosciences, China
Wei-Qiang Ji,
Institute of Geology and Geophysics
(CAS), China

*CORRESPONDENCE

Qiang Wang,
wqiang@gig.ac.cn
Xiu-Zheng Zhang,
zhangxz@gig.ac.cn

SPECIALTY SECTION

This article was submitted to
Geochemistry,
a section of the journal
Frontiers in Earth Science

RECEIVED 26 May 2022

ACCEPTED 02 August 2022

PUBLISHED 05 September 2022

CITATION

Xu C-B, Zeng J-P, Wang Q, Zhang X-Z,
Ou Q, Wang J, Hao L-L and Chen Y
(2022), Eocene adakitic quartz
monzonites and granite porphyries
from the northern Qiangtang Block,
central Tibet: Partial melting of
sediment-rich mélangé?
Front. Earth Sci. 10:953448.
doi: 10.3389/feart.2022.953448

COPYRIGHT

© 2022 Xu, Zeng, Wang, Zhang, Ou,
Wang, Hao and Chen. This is an open-
access article distributed under the
terms of the [Creative Commons
Attribution License \(CC BY\)](https://creativecommons.org/licenses/by/4.0/). The use,
distribution or reproduction in other
forums is permitted, provided the
original author(s) and the copyright
owner(s) are credited and that the
original publication in this journal is
cited, in accordance with accepted
academic practice. No use, distribution
or reproduction is permitted which does
not comply with these terms.

Eocene adakitic quartz monzonites and granite porphyries from the northern Qiangtang Block, central Tibet: Partial melting of sediment-rich mélangé?

Chuan-Bing Xu^{1,2}, Ji-Peng Zeng¹, Qiang Wang^{1,2,3*},
Xiu-Zheng Zhang^{1,3*}, Quan Ou¹, Jun Wang¹, Lu-Lu Hao¹ and
Yiwei Chen¹

¹State Key Laboratory of Isotope Geochemistry, Guangzhou Institute of Geochemistry, Chinese Academy of Sciences, Guangzhou, China, ²College of Earth and Planetary Sciences, University of Chinese Academy of Sciences, Beijing, China, ³CAS Center for Excellence in Deep Earth Science, Guangzhou, China

The timing and mechanism of crustal thickening and initial surface uplift of the Tibetan Plateau remain disputed. Here, we report zircon U–Pb geochronological and O isotopic and whole-rock geochemical and Sr–Nd isotopic data for Eocene (41–37 Ma) granite porphyries and quartz monzonites from the Qoima Co area of the northern Qiangtang Block, central Tibet. The granite porphyries are characterized by high silica content (72 wt%), adakitic trace-element compositions, enriched Sr–Nd isotope signatures [$(^{87}\text{Sr}/^{86}\text{Sr})_i = 0.7074$, $\epsilon\text{Nd}(t) = -4.5$], and a mean zircon $\delta^{18}\text{O}$ value of $+6.28 \pm 0.85\text{‰}$. The quartz monzonites exhibit high K_2O content (5.1–6.8 wt%) and $\text{K}_2\text{O}/\text{Na}_2\text{O}$ ratios (1.3–2.3). They also display adakitic geochemical characteristics, such as low Y (12–25 ppm) and Yb (1.1–1.8 ppm) content, high Sr/Y (98–187) and La/Yb (59–134) ratios, negligible Eu and positive Sr anomalies, and depletion in Nb and Ta. The quartz monzonites have $(^{87}\text{Sr}/^{86}\text{Sr})_i$ ratios ranging from 0.7069 to 0.7078, $\epsilon\text{Nd}(t)$ values of -5.1 to -2.9 , and mean $\delta^{18}\text{O}$ values ranging from $+6.27 \pm 0.64\text{‰}$ to $+7.91 \pm 0.32\text{‰}$. We suggest that the granite porphyries were most probably derived by the partial melting of thickened, sediment-bearing lower crust and that the quartz monzonites were most likely generated by the partial melting of sediment-rich mélangé. Combining these results with the existing tectonic and geophysical data, we conclude that continental subduction and mélangé underplating may have been responsible for crustal shortening and tectonic thickening.

KEYWORDS

adakitic rock, Eocene, thickened crust, Qiangtang Terrane, Tibetan Plateau

1 Introduction

The Tibetan Plateau is the world's highest and largest plateau and has the thickest continental crust (60–80 km; Yakovlev and Clark, 2014). However, the timing and mechanism of crustal thickening and initial surface uplift of the Tibetan Plateau are subjects of intense debate. Although most researchers agree that a Paleocene–Eocene protoplateau existed in central Tibet (Wang C. et al., 2008; Campbell et al., 2014; Wang et al., 2014), two main models have been proposed for its formation. The first model is that the southward subduction of Asian lithosphere beneath central Tibet kinetically drove protoplateau formation (Tapponnier et al., 2001; Wang Q. et al., 2008; Replumaz et al., 2016). The second model is that dense lithospheric mantle foundered to cause further uplift (Liu et al., 2008; Chen et al., 2013; Kelly et al., 2020; Zeng et al., 2021). Establishing the relative merits of these two models is of importance for understanding India–Asia continental tectonics (Replumaz et al., 2016 and Kelly et al., 2020, respectively).

Adakitic rocks are a geochemically distinct type of intermediate–felsic rocks with high Sr/Y and La/Yb ratios and low Y and Yb content, and they are commonly suggested to be derived from a plagioclase-free and garnet-bearing mafic source (Defant and Drummond, 1990; Gao et al., 2004; Castillo, 2012). Extensive Eocene high-K calc-alkaline adakitic magmatic rocks occur in the northern Qiangtang Block of central Tibet and were likely generated by the partial melting of the eclogitic crust from the subducted Songpan–Ganzi Block (Wang Q. et al., 2008, 2010; Long et al., 2015; Ou et al., 2017). However, Chen et al. (2013) and Zeng et al. (2021) also proposed that Eocene adakitic rocks were formed by the partial melting of the foundered and eclogitized lower crust of Qiangtang Block. Therefore, the genesis of these adakitic rocks remains unclear.

In this study, we report new geochronological and geochemical data for Eocene adakitic quartz monzonites and granite porphyries exposed in the Qoima Co area of the northern Qiangtang Block, central Tibet. These quartz monzonites exhibit clearly higher K₂O content and K₂O/Na₂O ratios compared with the high-K calc-alkaline high-K adakitic lavas from the northern Qiangtang Block (Wang Q. et al., 2008, 2010; Chen et al., 2013; Lai and Qin., 2013; Long et al., 2015; Ou et al., 2017; Zeng et al., 2021). Our new results reveal that the Qoima Co quartz monzonites were most probably generated by the partial melting of sediment-rich mélange. We suggest that continental subduction and mélange underplating were responsible for crustal shortening, tectonic thickening, and surface uplift of the central Tibetan Plateau.

2 Geological setting and sample descriptions

The Tibetan Plateau consists of five main blocks from south to north; that is, the Himalaya, Lhasa, Qiangtang,

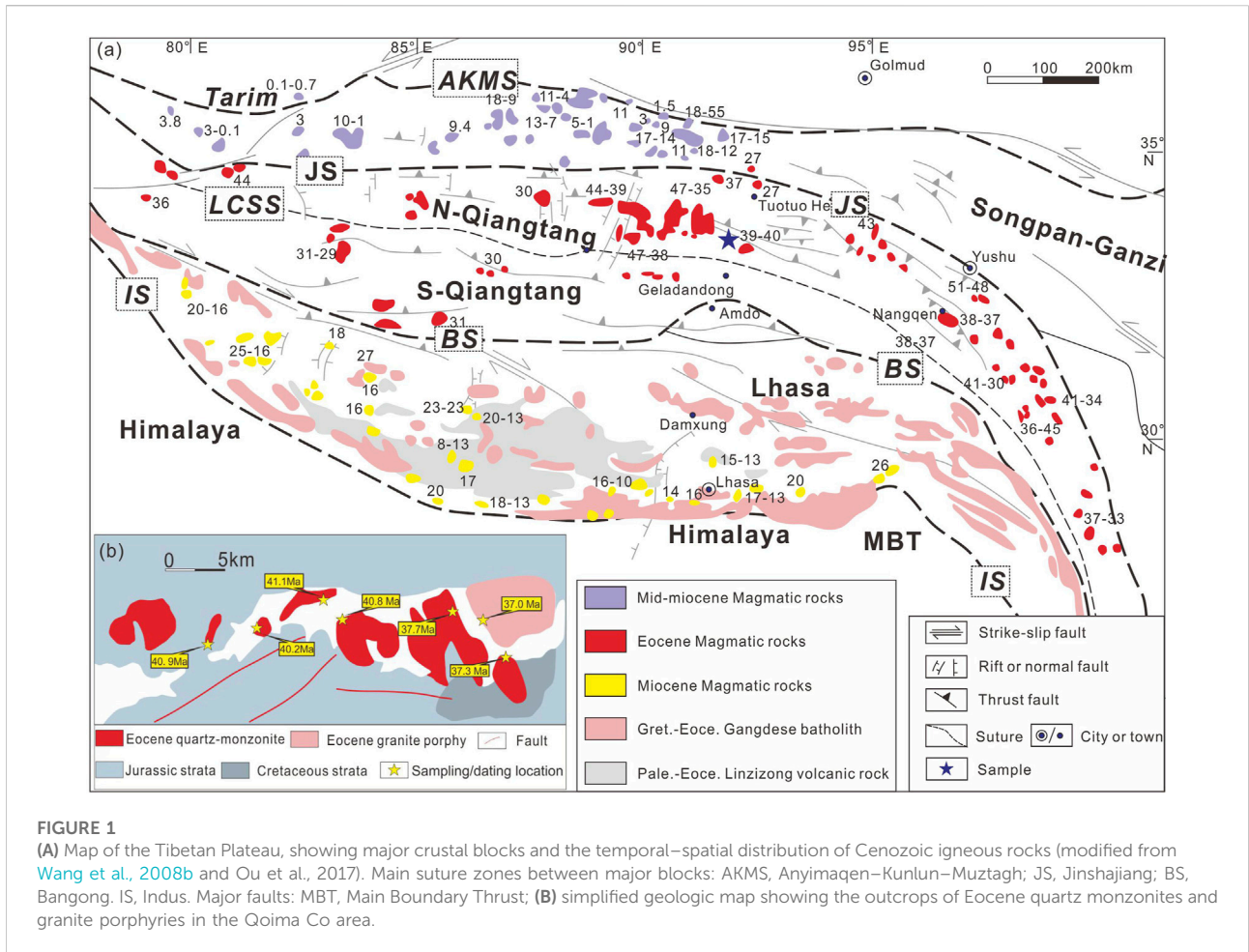
Songpan–Ganzi, and Kunlun–Qaidam blocks, which are separated by four main sutures (Figure 1A; Yin and Harrison, 2000; Wang C. et al., 2008). The Qiangtang Block is situated in the central Tibetan Plateau; the block is bounded by the Jinsha suture zone to the north and the Bangong–Nujiang suture zone to the south (Figure 1A; Yin and Harrison, 2000). Recent studies have argued that the Qiangtang Block can be subdivided into the southern and northern Qiangtang Blocks by the intervening Longmu Co–Shuanghu suture zone (Zhang et al., 2006; Metcalfe, 2013; Zhai et al., 2013), which is regarded as the remnant of the main Paleo-Tethys Ocean (Zhai et al., 2011; Metcalfe, 2013; Zhu et al., 2013). However, Kapp et al. (2000) suggested that it was a metamorphic core complex transported from the Jinsha Paleo-Tethyan subduction zone and exhumed during the Late Triassic period. Regardless, the Qiangtang Block had become an integrated, intracontinental block by the Early Cretaceous (Kapp and DeCelles, 2019).

In the northern Qiangtang Block, Cenozoic magmatic rocks are mainly distributed close to the Jinsha suture (Figure 1A), and their eruption ages range from ca. 51 to 0 Ma (Turner et al., 1996; Ding et al., 2003; Chung et al., 2005; Guo et al., 2006). The lavas exposed in the Duogecuoren and Zhentouya areas are dominated by shoshonitic in composition (Guo et al., 2006; Ding et al., 2007), some of which contain mafic and felsic granulite xenoliths (Hacker et al., 2000; Lai et al., 2011). However, recent studies indicated that most of these lavas are adakitic rocks. These adakitic rocks were interpreted to be generated by the partial melting of thickened lower crust (Lai et al., 2013; Long et al., 2015; Ou et al., 2017). Volcanic rocks of similar age are also exposed in the Tanggula, Fenghuoshan–Nangqian, and Yulinshan areas (Ding et al., 2003; Chung et al., 2005; Guo et al., 2006). In the southern Qiangtang Block, Cenozoic magmatic rocks are locally exposed in the Shuanghu, Ejumaima, and Nading Co areas, and they have eruption ages of 65 to 28 Ma (Ding et al., 2007).

The Qoima Co region is located in the northern Qiangtang Block, central Tibet. The intrusive rocks of Qoima Co comprise quartz monzonites and granite porphyries (Figure 1B). A total of 34 quartz monzonites and two granite porphyry samples were collected along a W–E-oriented transect through the Qoima Co region for petrological, geochemical, and geochronological analyses.

The whitish-gray quartz monzonites show medium porphyritic texture. Phenocrysts consist of K-feldspar (~35 vol%), plagioclase (~15 vol%), amphibole (~10 vol%), biotite (~8 vol%), and quartz (~5 vol%). The groundmass contains microcrystalline K-feldspar, plagioclase, and quartz (Figures 2A–D). Accessory minerals include zircon, apatite, titanite, and magnetite.

The Qoima Co granite porphyries are gray and massive, display porphyritic texture, and have similar constituent minerals to quartz monzonites, apart from a lack of amphibole. Phenocrysts consist of K-feldspar (~20 vol%),



plagioclase (~15 vol%), quartz (~15 vol%), and biotite (~5 vol%), all of which are set in a groundmass of microcrystalline K-feldspar, quartz, and plagioclase (Figures 2E,F). The accessory minerals include zircon and apatite.

3 Analytical results

The detailed analytical methods used during the study, including zircon U-Pb ages, whole rock major and trace element analyses, Sr-Nd isotope analyses, and zircon O isotope analyses, are presented in the Supplementary Material.

3.1 Zircon U-Pb ages

The LA-ICP-MS zircon U-Pb isotope data for the Qoima Co quartz monzonites and granite porphyries are compiled in Supplementary Table S1.

The zircon crystals from six quartz monzonite samples (14QW268, 14QW297-1, 14QW299-1, 14QW300-2,

14QW308-2, and 14QW312-2) are euhedral, show narrow oscillatory zoning, and range from 100 to 250 μm in length (Figures 3A-F). No inherited zircon grains were observed. The zircons have U content of 8–2,948 ppm, Th content of 7–4,315 ppm, and Th/U ratios of 0.2–3.7. Zircons from 14QW268, 14QW297-1, 14QW299-1, 14QW300-2, 14QW308-2, and 14QW312-2 yield a weighted mean ²⁰⁶Pb/²³⁸U ages of 40.9 ± 0.4 Ma (MSWD = 2.7; n = 22), 40.2 ± 0.3 Ma (MSWD = 0.77; n = 18), 40.8 ± 0.5 Ma (MSWD = 2.5; n = 19), 41.1 ± 0.7 Ma (MSWD = 3.6; n = 14), 37.7 ± 0.3 Ma (MSWD = 1.6; n = 20), and 37.0 ± 0.2 Ma (MSWD = 1.6; n = 16), respectively (Figures 3A-F). These ages represent the timing of crystallization of the quartz monzonites.

Zircon crystals from a single sample of granite porphyry (sample 14QW311-1) are long prismatic and 100–250 μm in length, and most have oscillatory zoning (Figure 3G). The zircons have U content of 525–3,190 ppm, Th content of 949–2,923 ppm, and Th/U ratios of 0.8–2.3. The analyses of 17 spots gave similar concordant ²⁰⁶Pb/²³⁸U ages varying from 37.9 to 36.1 Ma. These analyses yield a weighted mean ²⁰⁶Pb/²³⁸U age of 37.0 ± 0.2 Ma (MSWD = 1.6; n = 17; Figure 3G), which represents the

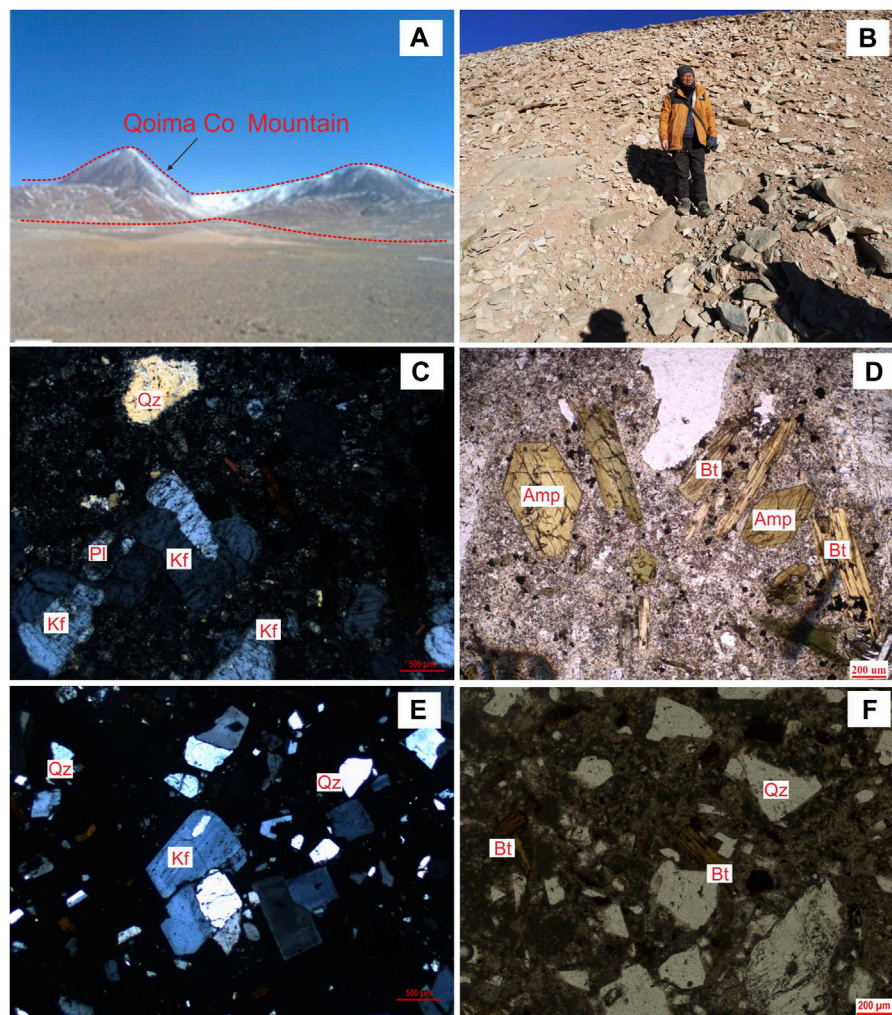


FIGURE 2

Field photographs and photomicrographs. (A) Goima Co Mountain; (B) Goima Co quartz monzonite; (C) porphyritic texture of quartz monzonite (cross-polarized light); (D) amphibole and biotite phenocrysts in quartz monzonite (plane-polarized light); (E) porphyritic texture of granite porphyry, showing K-feldspar phenocrysts (cross-polarized light). (F) biotite phenocrysts in granite porphyry (plane-polarized light). Mineral abbreviations: Pl, plagioclase; Kf, K-feldspar; Bt, biotite; Amp, amphibole; and Qtz, quartz.

crystallization age of the granite porphyry. Therefore, the Goima Co quartz monzonites and granite porphyry were formed during the Eocene period (41–37 Ma).

3.2 Major and trace elements

The results of major- and trace-element analyses of 34 samples from the Goima Co quartz monzonites and two samples from the Goima Co granite porphyries are listed in [Supplementary Table S2](#). The quartz monzonites have SiO₂ content ranging from 62 to 68 wt% (volatile-free), and plot in the alkaline field in a total-alkalis vs. silica (TAS) diagram ([Figure 4A](#)). The rocks are metaluminous to weakly

peraluminous, with A/CNK [molar ratio of Al₂O₃/(CaO + Na₂O + K₂O)] and A/NK [molar ratio of Al₂O₃/(Na₂O + K₂O)] ratios of 0.7–1.1 and 1.1–1.4, respectively ([Figure 5A](#)). They are shoshonitic ([Figure 4B](#)), with K₂O/Na₂O ratios of 1.3–2.3, and have wide variations in Mg# [molar MgO/(molar MgO + molar FeOT) × 100] of 15–59. The granite porphyries have an SiO₂ content of 72 wt% (volatile-free), and plot in the subalkaline ([Figure 4A](#)) and high-K calc-alkaline ([Figure 4B](#)) fields in discrimination diagrams. The rocks are peraluminous, with A/CNK ratios of 1.0–1.1, and plot in the peraluminous field ([Figure 5A](#)). In major-element Harker diagrams, the content of Fe₂O₃T, MgO, and CaO of the studied rocks decrease with increasing SiO₂, whereas Ti₂O, Al₂O₃, Na₂O, and P₂O₅ show no obvious relationship ([Figures 4C–H](#)).

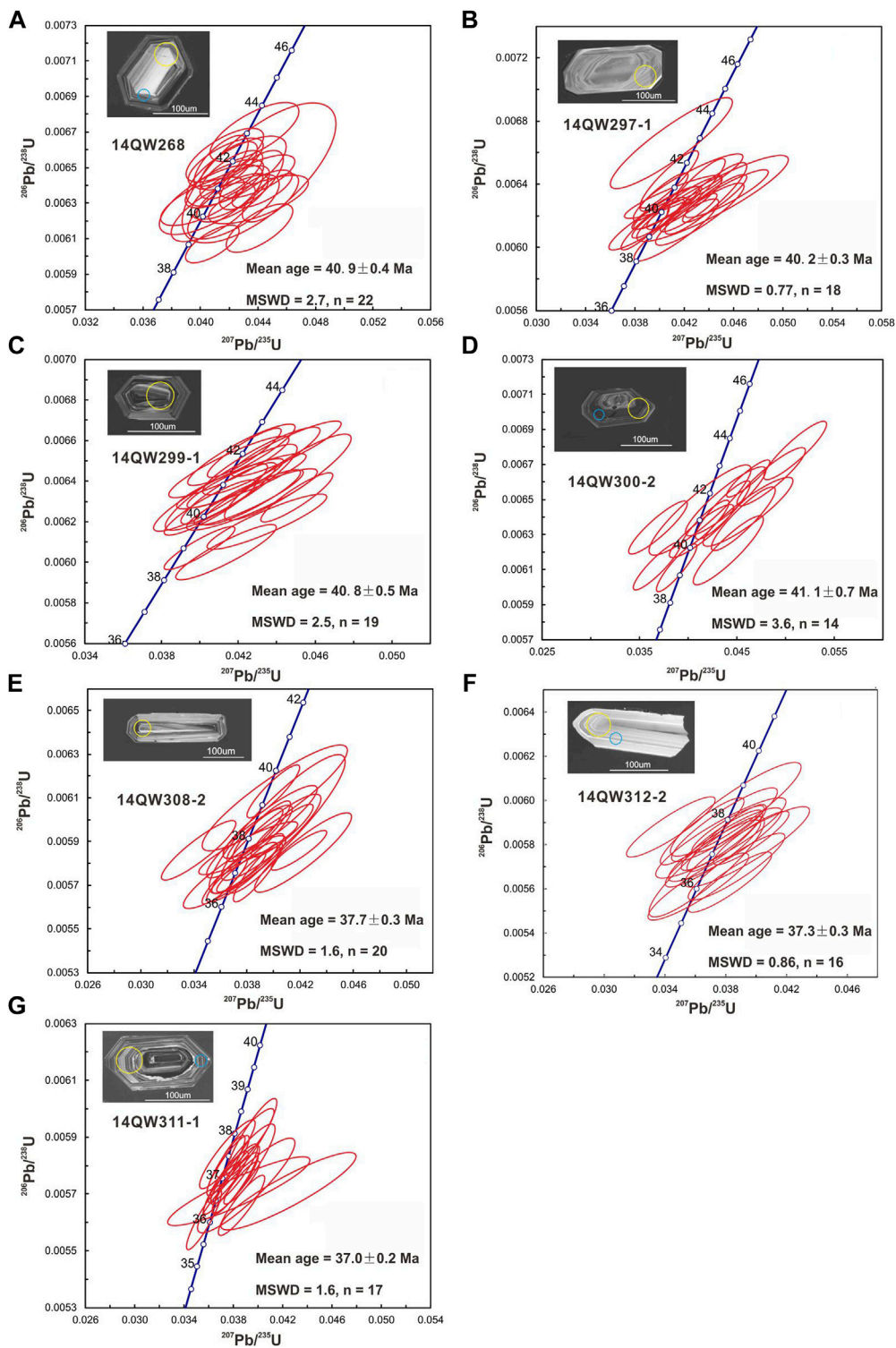


FIGURE 3

LA-ICP-MS U-Pb zircon age concordia diagrams for the studied Qoima Co igneous rocks, with the representative cathodoluminescence images of zircons. (A–F) Quartz monzonites; (G) granite porphyry. The yellow and blue circles on zircon CL images indicate the locations of U–Pb age sites and O isotope points, respectively.

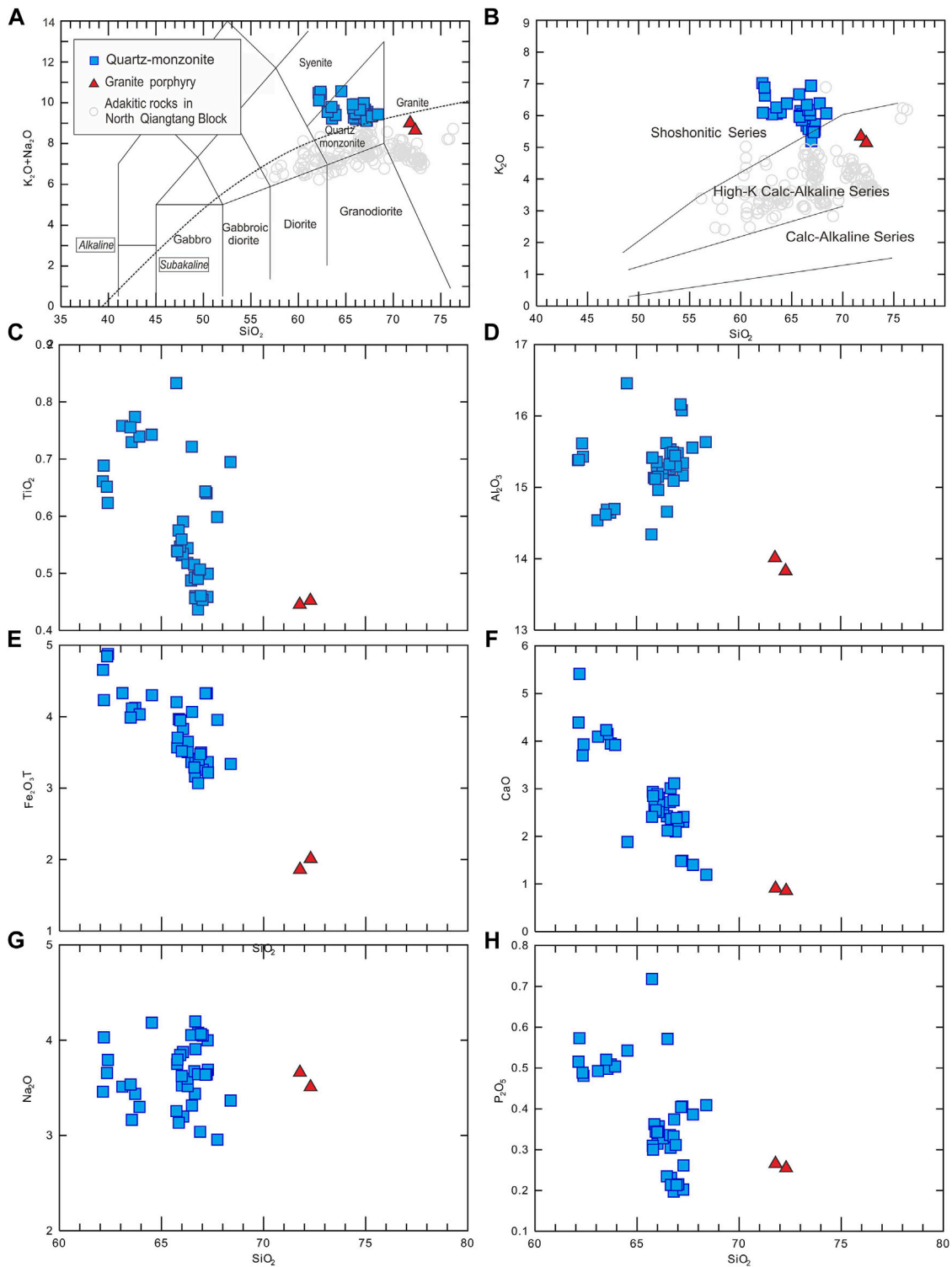
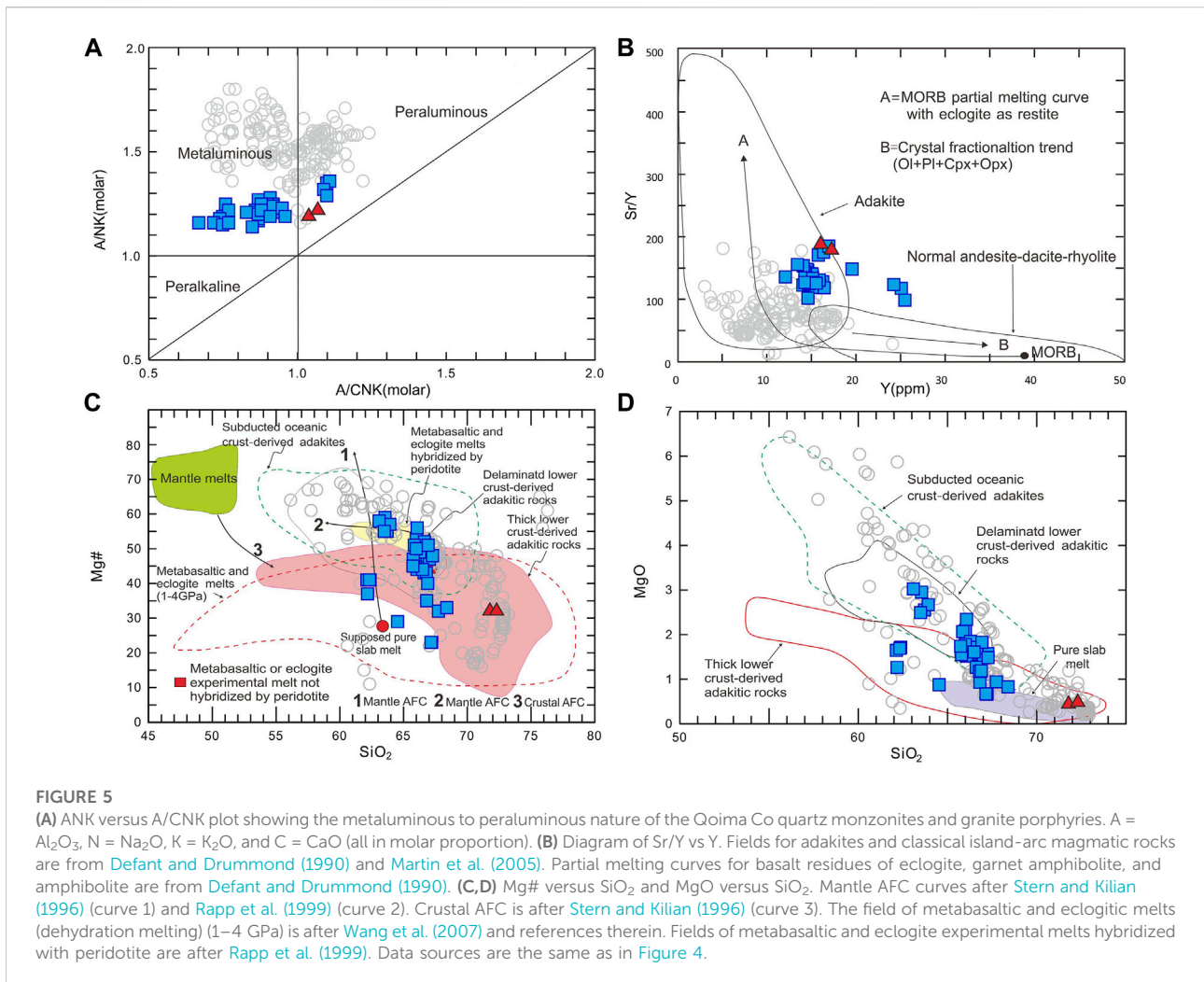


FIGURE 4

Major-element variation diagrams. (A) TAS classification diagram. All major-element data were recalculated to 100% on an LOI-free basis (Middlemost, 1994). (B–H) Harker diagrams. Data for northern Qiangtang Terrane adakitic rocks are from Wang Q. et al. (2008), Chen et al. (2013), Lai et al. (2013), Long et al. (2015), and Ou et al. (2017).



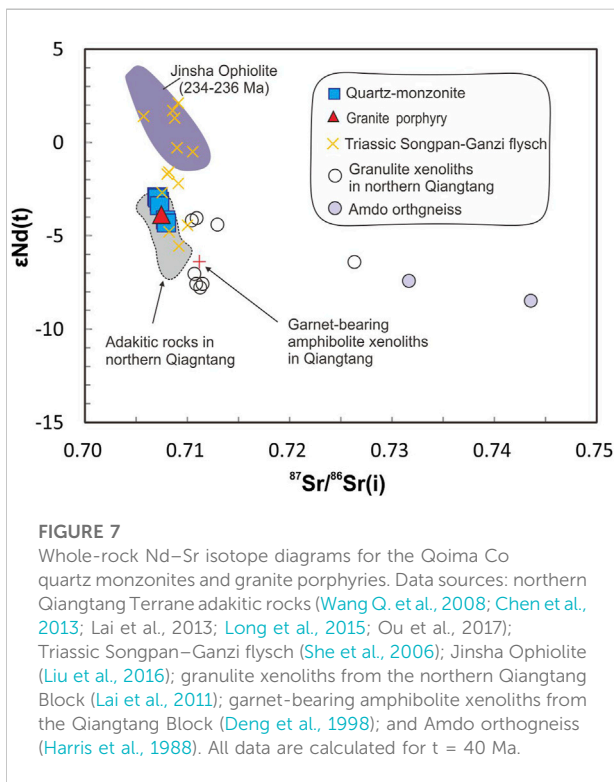
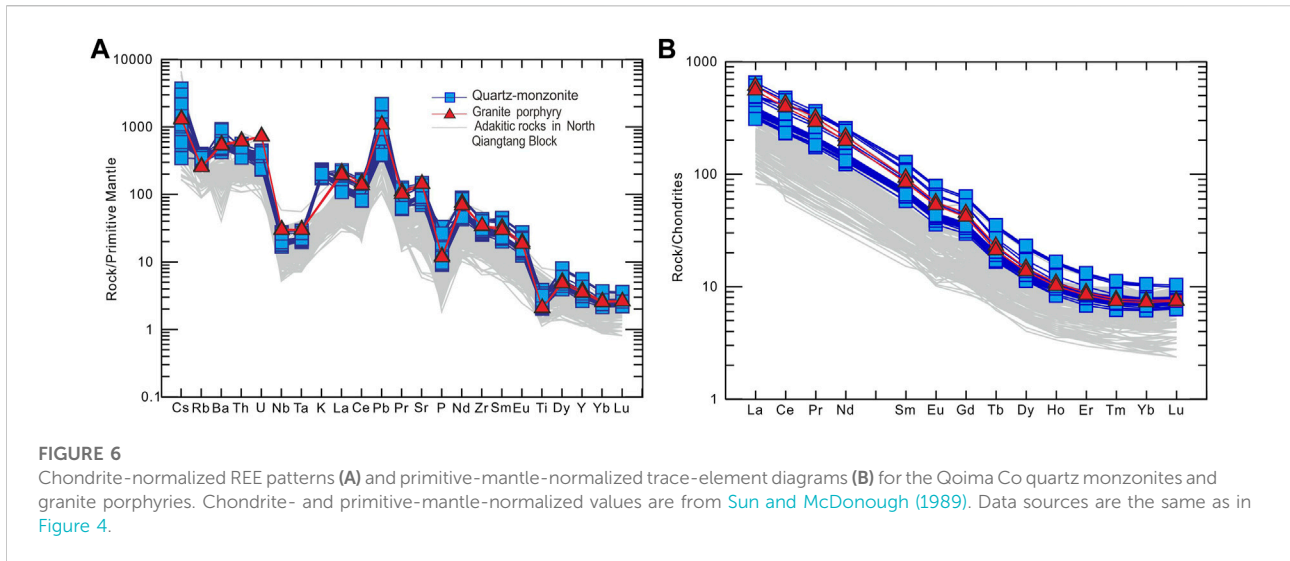
Both quartz monzonites and granite porphyries show similarities to adakitic rocks (Figure 5B), including their high Sr (1,469–3,104 ppm) and low Y (12–25 ppm) and Yb (1.1–1.8 ppm) content, together with their high La/Yb (59–134) and Sr/Y (98–184) ratios (Defant et al., 1990), negligible to positive Eu and Sr anomalies, and depletion in Nb, Ta, and Ti (Figures 6A,B). Compared with the contemporaneous Qiangtang Block adakitic rocks, the Qoima Co quartz monzonites and granite porphyries exhibit higher total-alkali (Figure 4B), K₂O (Figure 4B), Ba (Figure 9A), and Sr (Figure 9B) content.

The chondrite-normalized REE and primitive-mantle-normalized trace-element profiles of quartz monzonites and granite porphyries are highly similar (Figures 6A,B). Rocks from both intrusions display highly fractionated REE patterns, with La/Yb ratios of 59–134 and negligible negative Eu anomalies [Eu/Eu* = Eu_N/(Sm_N × Gd_N)^{1/2}] of 0.83–0.90. Both sets of rocks

show negative Nb, Ta, P, and Ti anomalies and positive Cs, U, Pb, and K anomalies (Figure 6A). The studied rocks also have high Ba (2,955–6,463 ppm) content.

3.3 Sr–Nd–O isotopes

Whole-rock Sr–Nd and zircon O isotope data for the Qoima Co quartz monzonites and granite porphyries are given in Supplementary Tables S3, S4. The quartz monzonites have initial ⁸⁷Sr/⁸⁶Sr ratios ranging from 0.7069 to 0.7078 and εNd (t) values from –5.1 to –2.9. The granite porphyries have an initial ⁸⁷Sr/⁸⁶Sr ratio of 0.7074 and an εNd (t) value of –4.5 (Figure 7). Zircons from the quartz monzonites have mean δ¹⁸O values of +6.27 ± 0.64‰ to +7.91 ± 0.32‰, and those from the granite porphyry have a mean δ¹⁸O value of +6.28 ± 0.85‰ (Figure 8).



4 Discussion

4.1 Petrogenesis of the Qoima Co adakitic granite porphyries

The results presented in Section 3 show that the adakitic granite porphyries from Qoima Co were formed during the early late Eocene period (ca. 37 Ma), and were therefore approximately

contemporaneous with late early Eocene to early late Eocene (48–37 Ma) adakitic rocks in the northern Qiangtang Block (Wang Q. et al., 2008, 2010; Chen et al., 2013; Lai et al., 2013; Long et al., 2015; Ou et al., 2017; Zeng et al., 2021). The Qiangtang Block had been in an intracontinental setting since the early Cretaceous (Pan et al., 2012; Zhu et al., 2013), which contrasts with the setting of typical adakites that are formed by the partial melting of subducted oceanic crust (Defant and Drummond, 1990). The high SiO₂ (~72 wt%) content of the Qoima Co adakitic granite porphyries suggests that they were not derived from direct partial melting of the mantle (Lloyd et al., 1985; Baker et al., 1995). The Qoima Co adakitic granite porphyries were also unlikely to have formed *via* assimilation–fractional crystallization of mantle-derived basaltic magmas on the basis of the following geochemical features and field observations of these rocks: 1) Mafic and ultramafic magmas have not been identified within the study areas or adjacent regions; and 2) the negligible Eu and positive Sr anomalies of granite porphyries indicate that they cannot have evolved from a mafic or ultramafic melt through substantial fractional crystallization of plagioclase. In addition, the Qoima Co adakitic granite porphyries may not have formed by the partial melting of delaminated lower crust, given their higher SiO₂ (~72 wt%) and lower MgO (~0.5 wt%) content relative to adakitic rocks derived from delaminated lower crust (Figure 5C; Wang et al., 2007).

The Qoima Co adakitic granite porphyries have the same MgO content and Mg# values as those of adakitic rocks derived from thickened lower crust and eclogite and metabasaltic experimental melts (Figures 5C,D; Wang et al., 2007). In addition, the samples have higher Ba and Sr content than those of high-K calc-alkaline high-K adakitic lavas from the northern Qiangtang Block (Figures 9A,B), and Zhang et al. (2019) suggested that postcollisional felsic magmatism with

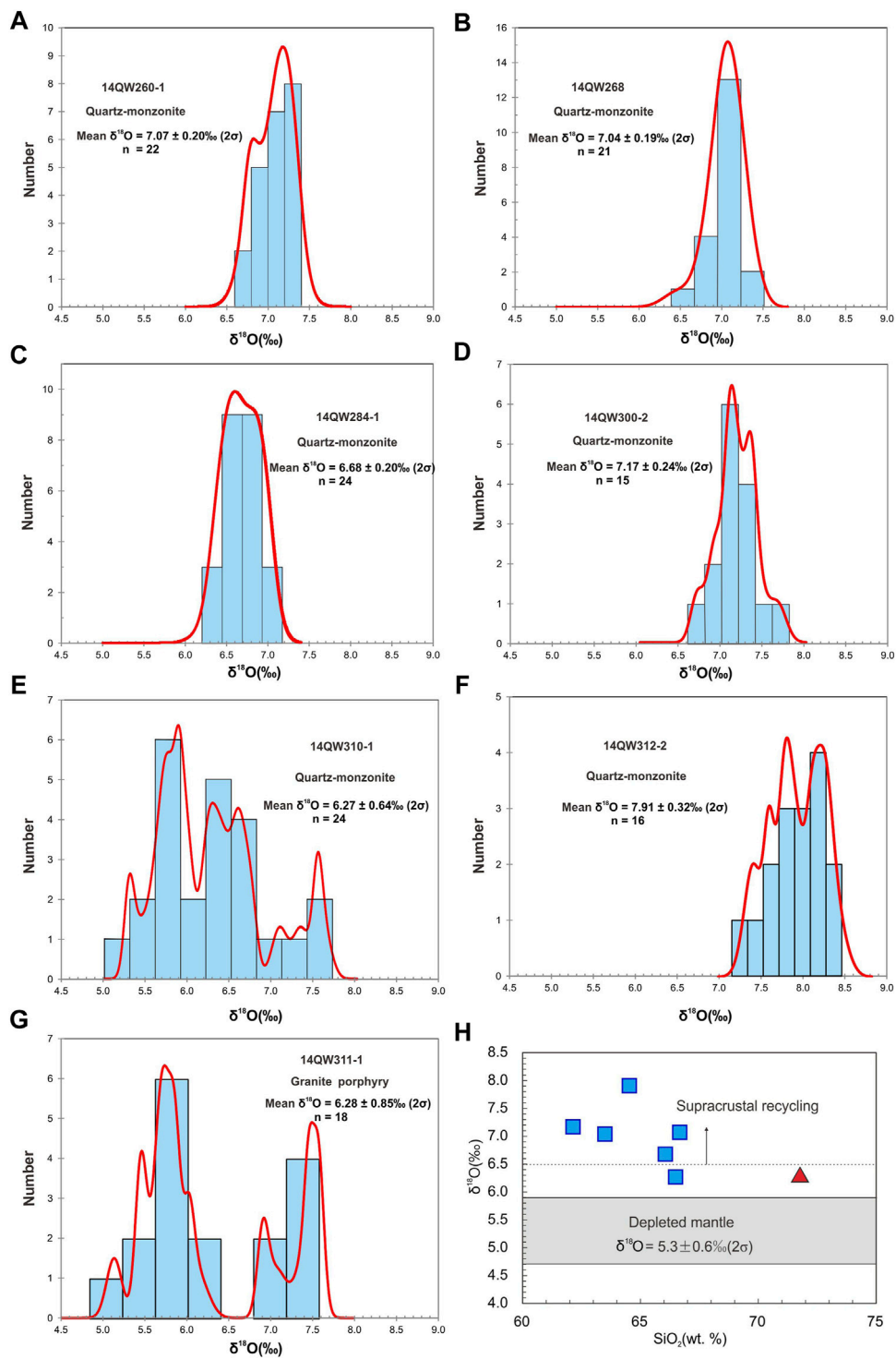
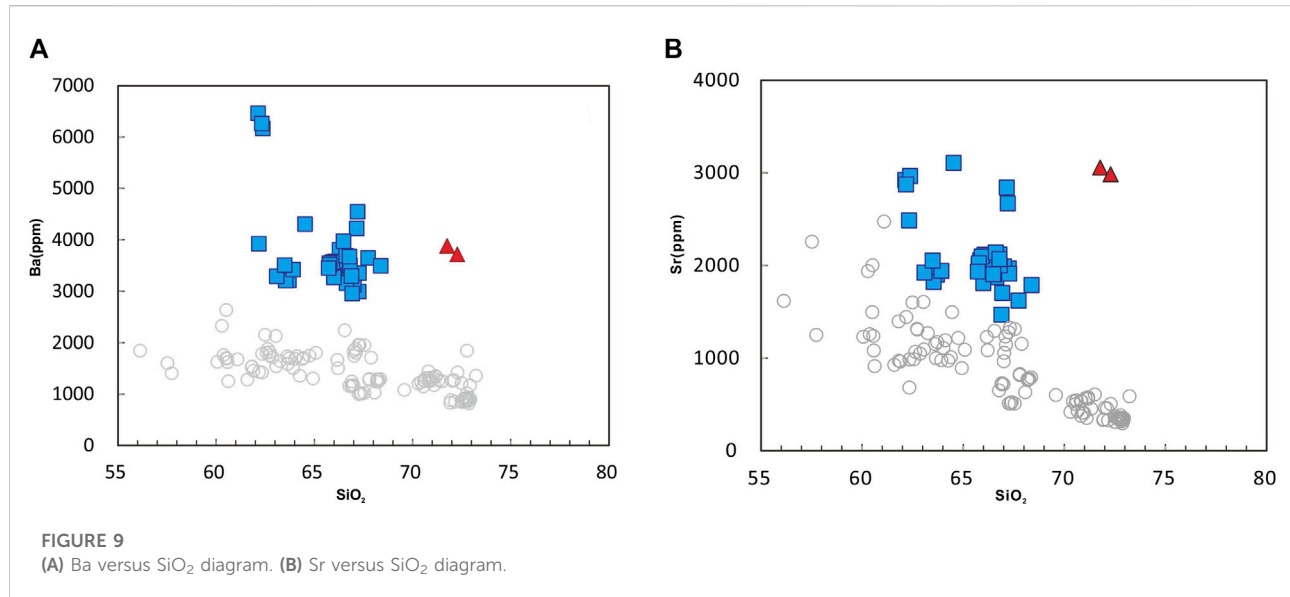


FIGURE 8

Histograms of zircon $\delta^{18}\text{O}$ values for (A–F) quartz monzonite and (G) granite porphyry. Red lines are the probability density curves. (H) $\delta^{18}\text{O}$ versus SiO_2 diagram. Zircons with $\delta^{18}\text{O} < 6.5\%$ (dashed line) are interpreted to have been formed from melts that contained a minor to negligible sedimentary component, whereas zircon $\delta^{18}\text{O}$ values $> 6.5\%$ indicate a substantial supracrustal material contribution (Cavosie et al., 2005; Valley et al., 2005).



high Ba and Sr characteristics may reflect a sediment contribution in their source region. In addition, the zircon $\delta^{18}\text{O}$ values of the Qoima Co adakitic granite porphyries ($6.28 \pm 0.85\text{‰}$) are higher than those of depleted mantle ($5.3 \pm 0.6\text{‰}$, 2σ ; Valley et al., 2005; Figures 8G,H), indicating the incorporation of supracrustal sediments that have interacted with the hydrosphere or hydrothermally altered magmatic rocks (Valley et al., 2005; Spencer et al., 2014). Therefore, we suggest that the Qoima Co adakitic granite porphyries were most likely derived by the partial melting of thickened, sediment-bearing lower crust.

4.2 Petrogenesis of the Qoima Co adakitic quartz monzonites

4.2.1 Origin of the Qoima Co adakitic quartz monzonitic magma

The Qoima Co quartz monzonites have high Sr content (1,469–3,104 ppm), low Y (12–25 ppm) and Yb (1.1–1.8 ppm) content, and high La/Yb (59–134) and Sr/Y (98–184) ratios, all of which are consistent with the geochemical characteristics of adakitic rocks (Figure 5B). Eocene high-K calc-alkaline adakitic magmatic rocks are extensively distributed in the northern Qiangtang Block of central Tibet. Three petrogenetic models have been proposed to explain the origin of these adakitic rocks; that is, the partial melting of 1) delaminated lower crust (Chen et al., 2013; Zeng et al., 2021), 2) subducted continental crust (Wang Q. et al., 2008; Jiang et al., 2011), and 3) thickened lower crust (Long et al., 2015; Ou et al., 2017). These three models are discussed with respect to the Qoima Co quartz monzonites.

Kay and Kay (1993) argued that the foundering or delamination of dense garnet-bearing mafic lower crust into the asthenosphere and subsequent interaction with the mantle peridotite could generate melts with high La/Yb and Sr/Y ratios beneath continental collisional orogens. However, the delamination of the mafic lower crust must be coupled with sinking of the subcontinental lithospheric mantle, which has a much greater thickness and density. Thus, delaminated material includes not only garnet-rich mafic lower crust but also the underlying subcontinental lithospheric mantle (Gao et al., 2007; Zeng et al., 2021). However, adakitic rocks formed in this way generally occur in within-plate extensional settings (Xu et al., 2002; Wang et al., 2006). In contrast, the presence of contraction basins and thrust faults (Figure 1A) suggests that the Qiangtang Block was undergoing crustal shortening in a compressional setting during the Eocene–Oligocene time (Tapponnier et al., 2001; Spurlin et al., 2005; Li et al., 2015; Kapp and DeCelles, 2019). In addition, the partial melting of (the residual or delaminated) lithospheric and/or upwelling of asthenospheric mantle can result in the emergence of other Mg-rich rock types, but large-scale mafic and ultramafic magmas have not been found within the study area or adjacent regions. Thus, it is highly improbable that the Qoima Co quartz monzonites were derived by the partial melting of delaminated lower crust.

Wang Q. et al. (2008) proposed that Eocene Duogecuoren adakitic lavas in the northern Qiangtang Block were formed by the partial melting of subducted continental crust. Low-Mg# (<45) peraluminous adakitic rocks are considered to have been derived by the partial melting of subducted sediment-dominated continent, and high-Mg# (>45) metaluminous adakitic rocks are considered to have resulted from the interaction of ascending

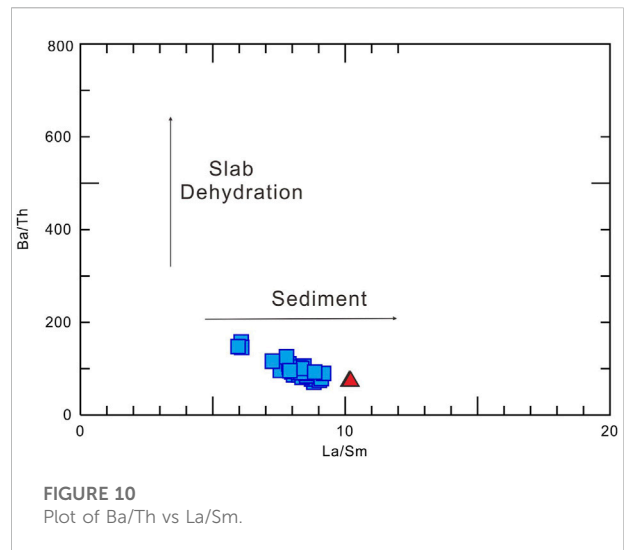
peraluminous melts with mantle peridotite. These adakitic lavas comprise high-K calc-alkaline andesites, dacites, and rhyolites. However, the intrusive rocks of Qoima Co comprise quartz monzonites and granite porphyries. The studied adakitic quartz monzonites are metaluminous to weakly peraluminous, and have variable Mg# values (15–59). The most striking feature is that the quartz monzonites have higher content of K₂O, Ba, and Sr (Figure 4B and Figures 9A,B), suggesting that the petrogenetic mechanism of adakitic quartz monzonites may be different from that of the Duogecuoren adakitic lavas.

The Qoima Co quartz monzonites have lower SiO₂ but higher K₂O, Al₂O₃, Fe₂O₃T, and CaO content than those of the granite porphyries (Figures 4B,D–F). Compared with the granite porphyries, the quartz monzonites have relatively high MgO (0.6–3.0 wt%), Cr (up to 128 ppm), and Ni (up to 75 ppm) content, suggesting the involvement of mantle peridotite. These characteristics suggest that the quartz monzonites cannot be originated from the thickened lower crust. In this study, the two groups of Qoima Co samples have overlapping trace element compositions (Figure 6) and Sr–Nd isotope signatures (Figure 7) and ages (Figure 3), indicating a petrogenetic link between the two groups. In addition, the Qoima Co quartz monzonites show complex elemental and isotopic compositions, with low Nb/La (0.11–0.19) ratios and unradiogenic Nd isotope compositions [ϵ Nd(t) = –5.1 to –2.9], which preclude significant involvement of asthenospheric mantle components. Therefore, we suggest that the Qoima Co quartz monzonites were most probably derived from a hybrid source composed of continental crust component and mantle wedge peridotite.

4.2.2 Nature of the Qoima Co adakitic quartz monzonitic magma sources

The quartz monzonites have felsic compositions, with SiO₂ content of 62–68 wt% and low MgO content of 0.66–3.02 wt% (volatile-free), suggesting that they were derived from the partial melting of mafic to felsic crustal lithologies rather than mafic–ultramafic mantle lithologies. The low ϵ Nd(t) (–5.1 to –2.9) and high initial ⁸⁷Sr/⁸⁶Sr (0.7069–0.7078) values overlap with those of adakitic rocks from the northern Qiangtang Block, which are typical continental crustal sources (Figure 7). Furthermore, quartz monzonites have Nb/U (2.8–1.4) and Ce/Pb (1.4–6.1) ratios that differ from those of OIB and MORB (Nb/U = ~47 and Ce/Pb = ~25; Hofmann et al., 1986), but resemble crustal values, further supporting their continental affinity. Therefore, mafic lower crust was most likely an end-member component in the magma source of the Qoima Co quartz monzonites.

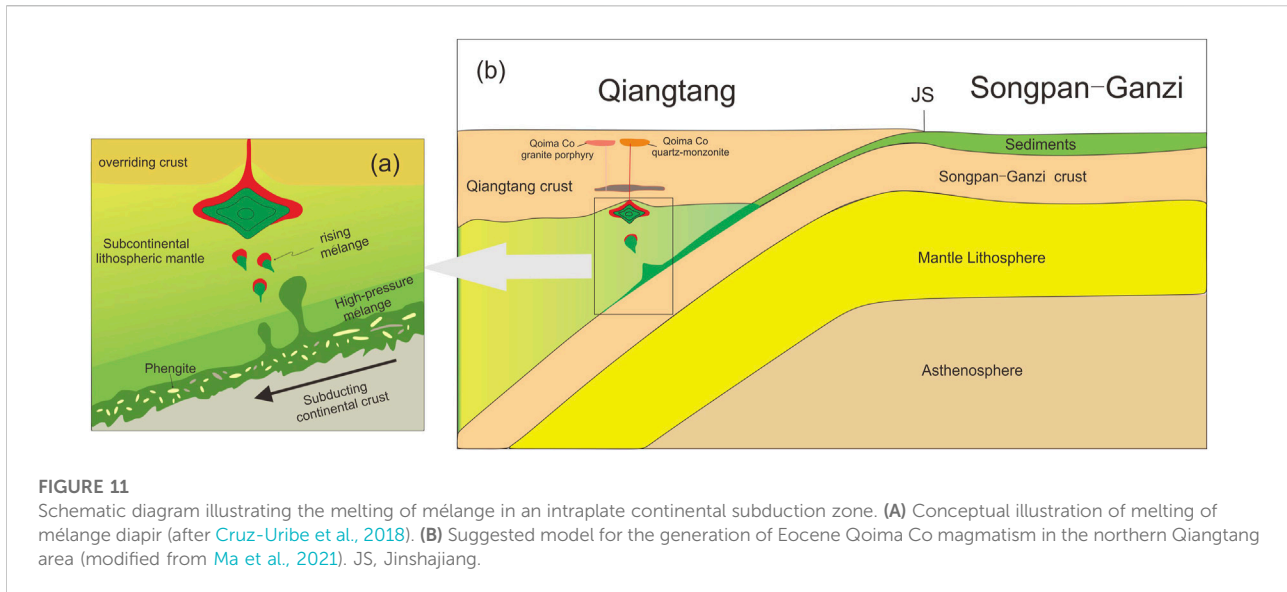
Several lines of evidence point to the involvement of sediments in the magma source of the Qoima Co quartz monzonites. First, these rocks have high Th (30–48 ppm) and Th/La (0.29–0.49) values that are similar to those of the upper continental crust or of the marine sediment (Plank and Langmuir, 1998; Plank, 2005),



suggesting that their source likely contained sediment (Hawkesworth et al., 1997; Plank, 2005; Wang Q. et al., 2008). In addition, most of the quartz monzonite samples have low Ba/Th and high La/Sm ratios (Figure 10), further suggesting the involvement of sediment. The samples have high Ba and Sr content (Figures 9A,B), and Zhang et al. (2019), which suggested that postcollisional felsic magmatism with high Ba and Sr may reflect the incorporation of sediment in their source region. Finally, the high zircon δ^{18} O values of the Qoima Co quartz monzonites (+6.27 ± 0.64‰ to +7.91 ± 0.32‰) (Figures 8A–F) suggest substantial incorporation of bulk sediment into their magma source, as aqueous fluids and small proportions of slab-derived melts cannot significantly change the O isotopic compositions of a magma source in the subduction zones (Eiler, 2001). Consequently, we suggest that sediments were incorporated into the magma source of the Qoima Co quartz monzonites.

Experimental data have shown that melts from the amphibolitic/basaltic lower continental crust are characterized by low Mg# values (<41), regardless of the degree of melting, whereas those with higher Mg# values can be generated only by the involvement of a mantle component (Rapp and Watson, 1995; Qian and Hermann, 2013). The studied samples have variable Mg# values (15–59) and MgO (0.66–3.02 wt%), Cr (15–128 ppm), and Ni (16–75 ppm) content. Consequently, we suggest that mantle wedge peridotite was most likely an end-member component in the magma source of the Qoima Co quartz monzonites.

Here, we further propose a mélangé source to explain the origin and compositional features of the Qoima Co quartz monzonites. Mélangé rocks have been proposed as a magmatic source in oceanic subduction zones (Marschall and Schumacher, 2012; Nielsen and Marschall, 2017), and are generated by mechanical mixing, metasomatic interactions, and diffusion under different P–T conditions (Guillot et al.,



2009; Bebout and Penniston-Dorland, 2016). Guo et al. (2013, 2014) used a mélangé model to explain the formation of postcollisional magmatic rocks in the Tibetan Plateau. Applying such a model to the present study, continental crust fragments with sediments are hypothesized to have been sheared downward by subducting crust to depths of ~80 km, where devolatilization took place (Menold et al., 2016) to form a mélangé source for the Qoima Co quartz monzonites (Figure 11).

The subcontinental lithospheric mantle is usually refractory under low geothermal gradients that exist in subduction zones (Zheng, 2012), whereas sediments have relatively low solidus temperatures at high pressure ($775 \pm 25^\circ\text{C}$ at 2 GPa) (Johnson and Plank, 2000). Experimental studies have shown that phengite-bearing eclogite undergoes dehydration melting at 1.5–2.0 GPa and $800\text{--}850^\circ\text{C}$ (Liu et al., 2019). Thus, a sediment-rich mélangé source would be more conducive to melting compared to a pure continental lithospheric mantle. The Qoima Co quartz monzonites have low Yb and high Sr content that are similar to those of coeval adakitic rocks from northern Qiangtang (Wang Q. et al., 2008; Long et al., 2015; Ou et al., 2017), which suggests a garnet-bearing and plagioclase-free source at depths of >50 km (Ma et al., 2021). The Qoima Co quartz monzonites also yield moderate zircon saturation thermometer (T_{Zr}) temperatures of $705\text{--}820^\circ\text{C}$ (Boehnke et al., 2013). The experimental results have suggested that melts produced from mechanical mixtures of basalt and sediment have compositions ranging from diorites to andesites to granodiorites, and it has been argued that intermediate to felsic rocks can be generated by the melting of sediment-rich mélangé in subduction zones (Castro et al., 2010; Marschall and Schumacher, 2012). These points together suggest that the partial melting of sediment-rich mélangé was involved in the formation

of the Qoima Co quartz monzonites during the continental collision.

5 Mélangé underplating and tectonic thickening

The Eocene magmatism induced by the continent–continent collision between the Eurasian and Indian plates recorded processes of crustal thickening and mountain building, meaning that the investigation of this magmatism is important in establishing the tectonic evolution of Tibet (Molnar et al., 1993; Yin and Harrison, 2000). As discussed previously, sediment-rich mélangé may have played an important role in the petrogenesis of the Qoima Co quartz monzonites. Given that the Sr–Nd isotopic compositions of the studied monzonites overlap the fields of Triassic Songpan–Ganzi flysch (Figure 6; She et al., 2006), we suggest that the sediment-rich mélangé was formed by the southward subduction of the Songpan–Ganzi Terrane. This interpretation is also consistent with the recent geophysical data, which support the occurrence of south-dipping continental subduction along the Jinsha suture (Tapponnier et al., 2001; Fu et al., 2010; Zhao et al., 2011).

Marschall and Schumacher (2012) provided an elegant physicochemical conceptual framework for the subduction zones that involve subduction channel mélanges in the recycling of trench sediments into the source of subduction-related magmas. Here, we adapt this model for the application to the northern Qiangtang Block geodynamic setting of converging subduction systems. We propose a two-stage petrogenetic model for the Qoima Co quartz monzonites. The first stage involves the formation of sediment-rich mélanges in the Songpan–Ganzi Terrane and Qiangtang subduction channels at the

slab–mantle interface as a consequence of the southward subduction of the Songpan–Ganzi continental lithosphere before the Eocene period (Figure 11B). The second stage of the model involves the diapiric transportation of buoyant, low-density, and enriched mélange domains into the shallow mantle. In combination with the adakitic characteristics of the Qoima Co quartz monzonites, we suggest that the mélange likely underplated the base of the Qiangtang lower crust (Figure 11A). Hence, we suggest that continental subduction and mélange underplating were responsible for Qiangtang crustal shortening and tectonic thickening, respectively.

6 Conclusion

This study used zircon U–Pb geochronological and O isotopic and whole-rock geochemical and Sr–Nd isotopic data for quartz monzonites and granite porphyries from the Qoima Co area of the northern Qiangtang Block, central Tibet, to constrain the timing and mechanism of crustal thickening and initial surface uplift of the Tibetan Plateau. The main conclusions of the study are as follows:

- 1) LA–ICP–MS zircon U–Pb dating shows that the Qoima Co quartz monzonites and granite porphyries in the northern Qiangtang Block were formed during the Eocene (41–37 Ma).
- 2) The granite porphyries are inferred to have been derived from the partial melting of thickened, sediment-bearing lower crust. The Qoima Co quartz monzonites are interpreted to have been derived through the partial melting of sediment-rich mélange.
- 3) Eocene continental subduction along the Jinsha suture and mélange underplating caused the shortening and thickening of the Qiangtang crust.

Data availability statement

The original contributions presented in the study are included in the article/Supplementary Material. Further inquiries can be directed to the corresponding author.

References

- Baker, M. B., Hirschmann, M. M., Ghiorso, M. S., and Stolper, E. M. (1995). Compositions of near-solidus peridotite melts from experiments and thermodynamic calculations. *Nature* 375, 308–311. doi:10.1038/375308a0
- Bebout, G. E., and Penniston-Dorland, S. C. (2016). Fluid and mass transfer at subduction interfaces—The field metamorphic record. *Lithos* 240, 228–258. doi:10.1016/j.lithos.2015.10.007
- Boehnke, P., Watson, E. B., Trail, D., Harrison, T. M., and Schmitt, A. K. (2013). Zircon saturation rerevisited. *Chem. Geol.* 351, 324–334. doi:10.1016/j.chemgeo.2013.05.028

Author contributions

QW initiated the study. QW, X-ZZ, and C-BX jointly designed the manuscript. QW, X-ZZ, C-BX, JW, and L-LH carried out petrological and geochemical interpretations and wrote the manuscript. QW, J-PZ, QO, and YC collected samples in the field. J-PZ and QO carried out zircon age. All authors approved the manuscript and agreed to submission.

Funding

Financial support for this research was provided by the National Natural Science Foundation of China (91855215 and 42021002) and the Second Tibetan Plateau Scientific Expedition and Research (STEP) (2019QZKK0702). This is contribution No. IS-3230 from GIGCAS.

Conflict of interest

The authors declare that the research was conducted in the absence of any commercial or financial relationships that could be construed as a potential conflict of interest.

Publisher's note

All claims expressed in this article are solely those of the authors and do not necessarily represent those of their affiliated organizations, or those of the publisher, the editors, and the reviewers. Any product that may be evaluated in this article, or claim that may be made by its manufacturer, is not guaranteed or endorsed by the publisher.

Supplementary material

The Supplementary Material for this article can be found online at: <https://www.frontiersin.org/articles/10.3389/feart.2022.953448/full#supplementary-material>

Campbell, I. H., Stepanov, A. S., Liang, H., Allen, C. M., Norman, M. D., Zhang, Y.-Q., et al. (2014). The origin of shoshonites: New insights from the tertiary high-potassium intrusions of eastern Tibet. *Contrib. Mineral. Pet.* 167, 983. doi:10.1007/s00410-014-0983-9

Castillo, R. (2012). Adakite petrogenesis. *Lithos* 134, 304–316. doi:10.1016/j.lithos.2011.09.013

Castro, A., Gerya, T., García-Casco, A., Fernández, C., Diaz-alvarado, J., Morenó-ventas, I., et al. (2010). Melting relations of MORB-sediment mélange in underplated mantle wedge plumes: implications for the origin of Cordilleran-type batholiths. *J. Pet.* 51, 1267–1295. doi:10.1093/petrology/egq019

- Cavosie, A. J., Valley, J. W., Wilde, S. A., and E. i. m. f. (2005). Magmatic $d^{18}O$ in 4400–3900 Ma detrital zircons: A record of the alteration and recycling of crust in the early archaean. *Earth Planet. Sci. Lett.* 235, 663–681. doi:10.1016/j.epsl.2005.04.028
- Chen, J., Wu, J., Xu, J., Dong, Y., Wang, B., and Kang, Z. (2013). Geochemistry of eocene high-mg# adakitic rocks in the northern qiangtang terrane, central tibet: Implications for early uplift of the plateau. *Geol. Soc. Am. Bull.* 125 (11–12), 1800–1819. doi:10.1130/B30755.1
- Chung, S.-L., Chu, M.-F., Zhang, Y., Xie, Y., Lo, C.-H., Lee, T.-Y., et al. (2005). Tibetan tectonic evolution inferred from spatial and temporal variations in post-collisional magmatism. *Earth. Sci. Rev.* 68 (3), 173–196. doi:10.1016/j.earscirev.2004.05.001
- Cruz-Uribe, A. M., Marschall, H. R., Gaetani, G. A., and Le Roux, V. (2018). Generation of alkaline magmas in subduction zones by partial melting of mélange diapirs—An experimental study. *Geology* 46, 343–346. doi:10.1130/G39956.1
- Defant, M. J., and Drummond, M. S. (1990). Derivation of some modern arc magmas by melting of young subducted lithosphere. *Nature* 347, 662–665. doi:10.1038/347662a0
- Deng, W.-M., Huang, X., and Zhong, D.-L. (1998). Alkali-rich porphyry and its relation with intraplate deformation of north part of Jinsha River belt in Western Yunnan, China. *Sci. China Ser. D. Earth Sci.* 41 (3), 297–305. doi:10.1007/BF02973119
- Ding, L., Kapp, P., Yue, Y. H., and Lai, Q. Z. (2007). Postcollisional calc-alkaline lavas and xenoliths from the southern Qiangtang terrane, central Tibet. *Earth Planet. Sci. Lett.* 254, 28–38. doi:10.1016/j.epsl.2006.11.019
- Ding, L., Kapp, P., Zhong, D., and Deng, W. (2003). Cenozoic volcanism in tibet: Evidence for a transition from oceanic to continental subduction. *J. Petrology* 44, 1833–1865. doi:10.1093/petrology/egg061
- Eiler, J. M. (2001). Oxygen isotope variations of basaltic lavas and upper mantle rocks. *Rev. Mineral. Geochem.* 43, 319–364. doi:10.2138/gsrmg.43.1.319
- Fu, Y.-V., Li, A., and Chen, Y.-J. (2010). Crustal and upper mantle structure of southeast Tibet from Rayleigh wave tomography. *J. Geophys. Res.* 115, B12323. doi:10.1029/2009JB007160
- Gao, S., Rudnick, R. L., Yuan, H. L., Liu, X. M., Liu, Y. S., Xu, W. L., et al. (2004). Recycling lower continental crust in the North China craton. *Nature* 432 (7019), 892–897. doi:10.1038/nature03162
- Gao, Y. F., Hou, Z. Q., Kamber, B. S., Wei, R. H., Meng, X. J., and Zhao, R. S. (2007). Adakite-like porphyries from the southern Tibetan continental collision zones: Evidence for slab melt metasomatism. *Contrib. Mineral. Pet.* 153, 105–120. doi:10.1007/s00410-006-0137-9
- Guillot, S., Hattori, K., Agard, P., Schwartz, S., and Vidal, O. (2009). Exhumation processes in oceanic and continental subduction contexts: A review. *Subduction Zone Geodyn.* 247, 175–205. doi:10.1007/978-3-540-87974-9_10
- Guo, Z. F., Wilson, M., Liu, J., and Mao, Q. (2006). Post-collisional, potassic and ultrapotassic magmatism of the northern Tibetan plateau: Constraints on characteristics of the mantle source, geodynamic setting and uplift mechanisms. *J. Pet.* 47 (6), 1177–1220. doi:10.1093/petrology/egl007
- Guo, Z., Wilson, M., Zhang, L., Zhang, M., Cheng, Z., and Liu, J. (2014). The role of subduction channel mélanges and convergent subduction systems in the petrogenesis of postcollisional K-rich mafic magmatism in NW Tibet. *Lithos* 198, 184–201. doi:10.1016/j.lithos.2014.03.020
- Guo, Z., Wilson, M., Zhang, M., Cheng, Z., and Zhang, L. (2013). Post-collisional, K-rich mafic magmatism in south tibet: Constraints on Indian slab-to-wedge transport processes and plateau uplift. *Contrib. Mineral. Pet.* 165, 1311–1340. doi:10.1007/s00410-013-0860-y
- Hacker, B. R., Gnos, E., Ratschbacher, L., Grove, M., McWilliams, M., Wan, J., et al. (2000). Hot and dry deep crustal xenoliths from tibet. *Science* 287, 2463–2466. doi:10.1126/science.287.5462.2463
- Harris, N., Ronghua, X., Lewis, C., Hawkesworth, C., and Yuquan, Z. (1988). Isotope geochemistry of the 1985 tibet geotraverse, Lhasa to golmud. *Phil. Trans. R. Soc. Lond. A* 327 (1594), 263–285. doi:10.1098/rsta.1988.0129
- Hawkesworth, C. J., Turner, S. P., McDermott, F., Peate, D. W., and van Calsteren, P. (1997). U–Th isotopes in arc magmas: Implications for element transfer from the subducted crust. *Science* 276, 551–555. doi:10.1126/science.276.5312.551
- Hofmann, A. W., Jochum, K. P., Seufert, M., and White, W. M. (1986). Nb and pb in oceanic basalts: New constraints on mantle evolution. *Earth Planet. Sci. Lett.* 79, 33–45. doi:10.1016/0012-821X(86)90038-5
- Jiang, Z.-Q., Wang, Q., Wyman, D. A., Tang, G.-J., Jia, X.-H., Yang, Y., et al. (2011). Origin of 30 Ma Chongmuda adakitic intrusive rocks in the southern Gangdese region, southern Tibet: Partial melting of the northward subducted Indian continent crust. *Geochimica* 40 (2), 126–146. doi:10.19700/j.0379-1726.2011.02.002
- Johnson, M. C., and Plank, T. (2000). Dehydration and melting experiments constrain the fate of subducted sediments. *Geochem. Geophys. Geosyst.* 1. doi:10.1029/1999GC000014
- Kapp, P., and DeCelles, P. G. (2019). Mesozoic–Cenozoic geological evolution of the Himalayan–Tibetan orogen and working tectonic hypotheses. *Am. J. Sci.* 319, 159–254. doi:10.2475/03.2019.01
- Kapp, P., Yin, A., Manning, C. E., Murphy, M., Harrison, T. M., Spurlin, M., et al. (2000). Blueschist-bearing metamorphic core complexes in the Qiangtang block reveal deep crustal structure of northern Tibet. *Geology* 28, 19–22. doi:10.1130/0091-7613(2000)028<0019:bbmcci>2.3.co;2
- Kay, R. W., and Kay, S. M. (1993). Delamination and delamination magmatism. *Tectonophysics* 219 (1), 177–189. doi:10.1016/0040-1951(93)90295-U
- Kelly, S., Beaumont, C., and Butler, J. P. (2020). Inherited terrane properties explain enigmatic postcollisional Himalayan–Tibetan evolution. *Geology* 48, 8–14. doi:10.1130/G46701.1
- Lai, S. C., and Qin, J. F. (2013). Adakitic rocks derived from the partial melting of subducted continental crust: Evidence from the Eocene volcanic rocks in the northern Qiangtang Block. *Gondwana Res.* 23 (2), 812–824. doi:10.1016/j.gr.2012.06.003
- Lai, S. C., Qin, J. F., and Grapes, R. (2011). Petrochemistry of granulite xenoliths from the cenozoic qiangtang volcanic field, northern Tibetan plateau: Implications for lower crust composition and Genesis of the volcanism. *Int. Geol. Rev.* 53, 926–945. doi:10.1080/00206810903334914
- Li, Y., Wang, C., Dai, J., Xu, G., Hou, Y., and Li, X. (2015). Propagation of the deformation and growth of the Tibetan–himalayan orogen: A review. *Earth. Sci. Rev.* 143, 36–61. doi:10.1016/j.earscirev.2015.01.001
- Liu, B., Ma, C. Q., Guo, Y. H., Xiong, F. H., Guo, P., and Zhang, X. (2016). Petrogenesis and tectonic implications of Triassic mafic complexes with MORB/OIB affinities from the Western Garzê-Litang ophiolitic mélange, central Tibetan Plateau. *Lithos* 260, 253–267. doi:10.1016/j.lithos.2016.06.009
- Liu, S., Hu, R.-Z., Feng, C.-X., Zou, H.-B., Li, C., Chi, X.-G., et al. (2008). Cenozoic high Sr/Y volcanic rocks in the Qiangtang terrane, northern Tibet: Geochemical and isotopic evidence for the origin of delaminated lower continental melts. *Geol. Mag.* 145 (4), 463–474. doi:10.1017/S0016756808004548
- Liu, W., Yang, Y., Busigny, V., and Xia, Q.-K. (2019). Intimate link between ammonium loss of phengite and the deep Earth's water cycle. *Earth Planet. Sci. Lett.* 513, 95–102. doi:10.1016/j.epsl.2019.02.022
- Lloyd, F. E., Arima, M., and Edgar, A. D. (1985). Partial melting of a phlogopite-clinopyroxene nodule from south-west Uganda: An experimental study bearing on the origin of highly potassic continental rift volcanics. *Contrib. Mineral. Pet.* 91, 321–329. doi:10.1007/BF00374688
- Long, X., Wilde, S. A., Wang, Q., Yuan, C., Wang, J. Li., Jiang, Z.-Q., et al. (2015). Partial melting of thickened continental crust in central Tibet: Evidence from geochemistry and geochronology of Eocene adakitic rhyolites in the northern Qiangtang Terrane. *Earth Planet. Sci. Lett.* 414, 30–44. doi:10.1016/j.epsl.2015.01.007
- Ma, Lin., Gng, A., Ack, C., Qiang, W., Gjwa, B., Jhy, E., et al. (2021). B isotopes reveal eocene mélange melting in northern tibet during continental subduction. *Lithos* 392–393, 106146. doi:10.1016/j.lithos.2021.106146
- Marschall, H. R., and Schumacher, J. C. (2012). Arc magmas sourced from mélange diapirs in subduction zones. *Nat. Geosci.* 5, 862–867. doi:10.1038/ngeo1634
- Martin, H., Smithies, R. H., Rapp, R., Moyen, J. F., and Champion, D. (2005). An overview of adakite, tonalite-trondjemite-granodiorite (TTG), and sanukitoid: Relationships and some implications for crustal evolution. *Lithos* 79, 1–24. doi:10.1016/j.lithos.2004.04.048
- Menold, C. A., Grove, M., Sievers, N. E., Manning, C. E., Yin, A., Young, E. D., et al. (2016). Argon, oxygen, and boron isotopic evidence documenting 40ArE accumulation in phengite during water-rich high-pressure subduction metasomatism of continental crust. *Earth Planet. Sci. Lett.* 446, 56–67. doi:10.1016/j.epsl.2016.04.010
- Metcalfe, I. (2013). Gondwana dispersion and Asian accretion: Tectonic and palaeogeographic evolution of eastern Tethys. *J. Asian Earth Sci.* 66, 1–33. doi:10.1016/j.jseas.2012.12.020
- Molnar, P., England, P., and Martinod, J. (1993). Mantle dynamics, uplift of the Tibetan plateau, and the Indian monsoon. *Rev. Geophys.* 31, 357–396. doi:10.1029/93RG02030
- Nielsen, S. G., and Marschall, H. R. (2017). Geochemical evidence for mélange melting in global arcs. *Sci. Adv.* 3, e1602402. doi:10.1126/sciadv.1602402

- Plank, T. (2005). Constraints from Thorium/Lanthanum on sediment recycling at subduction zones and the evolution of the continents. *J. Pet.* 46 (5), 921–944. doi:10.1093/petrology/egi005
- Plank, T., and Langmuir, C. H. (1998). The chemical composition of subducting sediment and its consequences for the crust and mantle. *Chem. Geol.* 145, 325–394. doi:10.1016/S0009-2541(97)00150-2
- Qian, Q., and Hermann, J. (2013). Partial melting of lower crust at 10–15 kbar: Constraints on adakite and TTG formation. *Contrib. Mineral. Pet.* 165, 1195–1224. doi:10.1007/s00410-013-0854-9
- Rapp, R. P., Shimizu, N., Norman, M. D., and Applegate, G. S. (1999). Reaction between slab-derived melts and peridotite in the mantle wedge: Experimental constraints at 3.8 GPa. *Chem. Geol.* 160, 335–356. doi:10.1016/S0009-2541(99)00106-0
- Rapp, R. P., and Watson, E. B. (1995). Dehydration melting of metabasalt at 8–32 kbar: Implications for continental growth and crust-mantle recycling. *J. Petrology* 36, 891–931. doi:10.1093/petrology/36.4.891
- Replumaz, A., Funicello, F., Reitano, R., Faccenna, C., and Balon, M. (2016). Asian collisional subduction: A key process driving formation of the Tibetan plateau. *Geology* 44, 943–946. doi:10.1130/G38276.1
- She, Z. B., Ma, C. Q., Mason, R., Li, J. W., Wang, G. C., and Lei, Y. H. (2006). Provenance of the triassic songpan-ganzi flysch, west China. *Chem. Geol.* 231, 159–175. doi:10.1016/j.chemgeo.2006.01.001
- Spencer, C. J., Cawood, P. A., Hawkesworth, C. J., Raub, T. D., Prave, A. R., and Roberts, N. M. (2014). Proterozoic onset of crustal reworking and collisional tectonics: Reappraisal of the zircon oxygen isotope record. *Geology* 42, 451–454. doi:10.1130/G35363.1
- Spurlin, M. S., Yin, A., Horton, B. K., Zhou, J., and Wang, J. (2005). Structural evolution of the Yushu-Nangqian region and its relationship to syn-collisional igneous activity, east-central Tibet. *Geol. Soc. Am. Bull.* 117 (9–10), 1293–1317. doi:10.1130/B25572.1
- Stern, C. R., and Kilian, R. (1996). Role of the subducted slab, mantle wedge and continental crust in the generation of adakites from the Andean Austral Volcanic Zone. *Contributions Mineralogy Petrology* 123, 263–281. doi:10.1007/s004100050155
- Sun, S.-S., and McDonough, W. (1989). Chemical and isotopic systematics of oceanic basalts: Implications for mantle composition and processes. *Geol. Soc. Lond. Spec. Publ.* 42 (1), 313–345. doi:10.1144/GSL.SP.1989.042.01.19
- Tapponnier, P., Zhiqin, X., Roger, F., Meyer, B., Arnaud, N., Wittlinger, G., et al. (2001). Oblique stepwise rise and growth of the Tibet plateau. *Science* 294 (5547), 1671–1677. doi:10.1126/science.105978
- Valley, J. W., Lackey, J. S., Cavosie, A. J., Clechenko, C. C., Spicuzza, M. J., Basei, M. A. S., et al. (2005). 4.4 billion years of crustal maturation: Oxygen isotope ratios of magmatic zircon. *Contrib. Mineral. Pet.* 150, 561–580. doi:10.1007/s00410-005-0025-8
- Wang, C., Dai, J., Zhao, X., Li, Y., Graham, S. A., He, D., et al. (2014). Outward-growth of the Tibetan plateau during the Cenozoic: A review. *Tectonophysics* 621, 1–43. doi:10.1016/j.tecto.2014.01.036
- Wang, C., Zhao, X., Liu, Z., Lippert, P. C., Graham, S. A., Coe, R. S., et al. (2008a). Constraints on the early uplift history of the Tibetan Plateau. *Proc. Natl. Acad. Sci. U. S. A.* 105 (13), 4987–4992. doi:10.1073/pnas.0703595105
- Wang, Q., Hawkesworth, C. J., Wyman, D., Chung, S. L., Wu, F. Y., Li, X. H., et al. (2016). Pliocene–Quaternary crustal melting in central and northern Tibet and insights into crustal flow. *Nat. Commun.* 7, 11888. doi:10.1038/ncomms11888
- Wang, Q., Li, J. W., Jian, P., Zhao, Z. H., Xiong, X. L., Bao, Z. W., et al. (2005a). Alkaline syenites in eastern Cathaysia (south China): Link to Permian–Triassic transtension. *Earth Planet. Sci. Lett.* 230 (3–4), 339–354. doi:10.1016/j.epsl.2004.11.023
- Wang, Q., McDermott, F., Xu, J. F., Bellon, H., and Zhu, Y. T. (2005b). Cenozoic K-rich adakitic volcanic rocks in the Hohxil area, northern Tibet: Lower-crustal melting in an intracontinental setting. *Geol.* 33, 465–468. doi:10.1130/G21522.1
- Wang, Q., Wyman, D. A., Li, Z.-X., Sun, W., Chung, S.-L., Vasconcelos, P. M., et al. (2010). Eocene north–south trending dikes in central Tibet: New constraints on the timing of east–west extension with implications for early plateau uplift? *Earth Planet. Sci. Lett.* 298 (1), 205–216. doi:10.1016/j.epsl.2010.07.046
- Wang, Q., Wyman, D. A., Xu, J.-F., Dong, Y., Vasconcelos, P. M., Pearson, N., et al. (2008b). Eocene melting of subducting continental crust and early uplifting of central Tibet: Evidence from central-Western Qiangtang high-K calc-alkaline andesites, dacites and rhyolites. *Earth Planet. Sci. Lett.* 272 (1), 158–171. doi:10.1016/j.epsl.2008.04.034
- Wang, Q., Wyman, D. A., Xu, J., Jian, P., Zhao, Z., Li, C., et al. (2007). Early Cretaceous adakitic granites in the northern Dabie complex, central China: Implications for partial melting and delamination of thickened lower crust. *Geochim. Cosmochim. Acta* 71 (10), 2609–2636. doi:10.1016/j.gca.2007.03.008
- Wang, Q., Xu, J.-F., Jian, P., Bao, Z.-W., Zhao, Z.-H., Li, C.-F., et al. (2006). Petrogenesis of adakitic porphyries in an extensional tectonic setting, Dexing, South China: Implications for the Genesis of porphyry copper mineralization. *J. Pet.* 47 (1), 119–144. doi:10.1093/petrology/egi070
- Xiong, X. L., Adam, J., and Green, T. H. (2005). Rutile stability and rutile/melt HFSE partitioning during partial melting of hydrous basalt: Implications for TTG Genesis. *Chem. Geol.* 218, 339–359. doi:10.1016/j.chemgeo.2005.01.014
- Xu, J.-F., Shinjo, R., Defant, M. J., Wang, Q., and Rapp, R. P. (2002). Origin of Mesozoic adakitic intrusive rocks in the Ningzhen area of east China: Partial melting of delaminated lower continental crust? *Geol.* 30 (12), 1111–1114. doi:10.1130/0091-7613(2002)030<1111:oomair>2.0.co;2
- Yin, A., and Harrison, T. M. (2000). Geologic evolution of the Himalayan–Tibetan orogen. *Annu. Rev. Earth Planet. Sci.* 28 (1), 211–280. doi:10.1146/annurev.earth.28.1.211
- Zeng, Y., Ducea, M. N., Xu, J., Chen, J., and Dong, Y. H. (2021). Negligible surface uplift following foundering of thickened central Tibetan lower crust. *Geology* 49 (1), 45–50. doi:10.1130/G48142.1
- Zhai, Q.-G., Jahn, B.-M., Wang, J., Su, L., Mo, X.-X., Wang, K.-L., et al. (2013). The Carboniferous ophiolite in the middle of the Qiangtang terrane, northern Tibet: SHRIMP U–Pb dating, geochemical and Sr–Nd–Hf isotopic characteristics. *Lithos* 168–169 (3), 186–199. doi:10.1016/j.lithos.2013.02.005
- Zhang, K.-J., Zhang, Y.-X., Li, B., Zhu, Y.-T., and Wei, R.-Z. (2006). The blueschist-bearing Qiangtang metamorphic belt (northern Tibet, China) as an *in situ* suture zone: Evidence from geochemical comparison with the Jinsha suture. *Geol.* 34, 493–496. doi:10.1130/G22404.1
- Zhang, L., Zhang, H., Hawkesworth, C., Luo, B., Yang, H., Xu, W., et al. (2019). Sediment contribution in post-collisional high Ba–Sr magmatism: Evidence from the Xijing pluton in the Alxa block, NW China. *Gondwana Res.* 69, 177–192. doi:10.1016/j.gr.2018.12.010
- Zhao, W., Kumar, P., Mechie, J., Kind, R., Meissner, R., Wu, Z., et al. (2011). Tibetan plate overriding the Asian plate in central and northern Tibet. *Nat. Geosci.* 4 (12), 870–873. doi:10.1038/ngeo1309
- Zheng, Y.-F. (2012). Metamorphic chemical geodynamics in continental subduction zones. *Chem. Geol.* 328, 5–48. doi:10.1016/j.chemgeo.2012.02.005
- Zhu, D.-C., Zhao, Z.-D., Niu, Y., Dilek, Y., Hou, Z.-Q., and Mo, X.-X. (2013). The origin and pre-Cenozoic evolution of the Tibetan Plateau. *Gondwana Res.* 23 (4), 1429–1454. doi:10.1016/j.gr.2012.02.002